Available online at www.sciencedirect.com
ScienceDirect
Ceramics International 34 (2008) 385–389
CERAMICS INTERNATIONAL
www.elsevier.com/locate/ceramint

In situ measurement and simulation of temperature and stress gradients during sintering of large ceramic components

F. Raether *, A. Klimera, J. Baber

Fraunhofer Institute for Silicate Research, Neunerplatz 2, 97082 Würzburg, Germany

Received 25 September 2006; received in revised form 30 September 2006; accepted 26 October 2006
Available online 16 January 2007

Abstract

A special thermooptical measuring system was used to determine mechanical, thermal and sintering properties during firing simultaneously. Combining customary and novel in situ measuring methods, a complete dataset was obtained which includes elastic and viscous moduli, thermal conductivity and coefficients of heat transfer, specific heat, reaction and sintering data and gas permeability. Using finite element methods (FEM) the temperature fields in large components were simulated for various time temperature cycles. From the temperature field local reaction and shrinkage rates were calculated. The corresponding stresses were obtained using FEM again. The time temperature cycle was optimized taking into account both a sufficient safety margin to the respective strength of the sintering material and the economic requirement for a short firing cycle. The use of the methods was demonstrated considering as example a large high voltage porcelain insulator, which undergoes a number of phase transformations during firing.

Keywords: A. Firing; High voltage insulator; Stress; Simulation

1. Introduction

Thermal conductivity in ceramic green parts is unfavorably small. During heating large temperature gradients can arise, producing thermal stresses. Gaseous species which are released during heating, e.g. organics during debinding, cause local overpressure and additional stresses. To avoid defects during firing, the time–temperature cycle and the furnace atmosphere has to be carefully matched to the demands of the specific component. Optimization of these process parameters by trial and error is laborious and inefficient. Due to the large number of parameters and their large interaction, even methods of experimental design often fail.

Various mechanical, thermal and thermochemical material data are required to achieve a quantitative prediction of temperature and stress fields within the components: Elastic and viscous moduli, thermal conductivity, specific heat, reaction data like activation energies, data on sintering kinetics and gas permeability. Most of these data are obtained by in situ measurements in a lab furnace. The transferability of the conditions determined in the lab furnace to the production furnace is a precondition for a successful development. This requires well-defined temperatures and atmospheres in the lab furnace which can be varied in the same range as in the respective industrial furnace.

At Fraunhofer ISC a novel type of non-contact in situ measuring methods has been developed which is applied in closed furnaces with variable atmospheres using samples in the range of some centimeters. The paper presents an application of these thermooptical measuring methods (TOM) to reduce the firing cycle of high voltage insulators.

2. Experimental procedure

Green samples were made by rod extrusion of a compound for an alumina porcelain used in high voltage insulators (C120). Cylindrical samples, which had a diameter of 22 mm and a height of 3 or 15 mm (for laser-flash and creep measurements respectively) were prepared from larger parts by turning and sawing. Green density was 1.94 g/cm^3.

* Corresponding author. Tel.: +49 931 4100 200; fax: +49 931 4100 299.
E-mail addresses: raether@isc.fhg.de (F. Raether), klimera@isc.fhg.de (A. Klimera), baber@isc.fhg.de (J. Baber).

0272-8842/$34.00
doi:10.1016/j.ceramint.2006.10.025

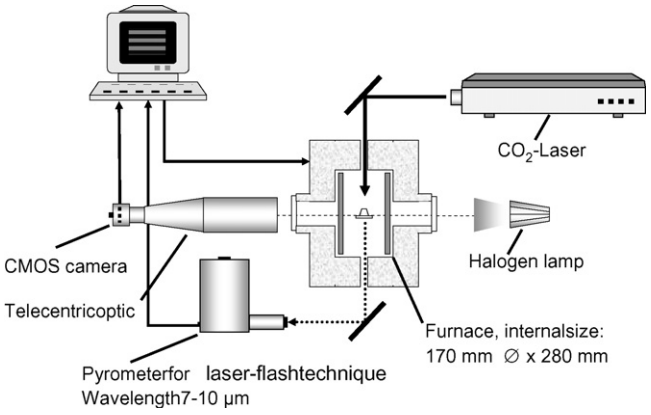

Fig. 1. Setup of thermooptical measuring device (TOM).

Fig. 1 shows the setup of TOM, which allows a simultaneous in situ measurement of shrinkage, warpage, creep and heat transfer during sintering. A resistance heated hood-type lab furnace in a water cooled and vacuum tight stainless steel box was used. Heaters were made from $MoSi_2$. Alumina fiber board was used for thermal insulation. Gas flow was controlled by a mixing unit, which was driven by a PC. Previous experiments showed that sintering behavior of porcelain changes considerably between dry and moist furnace atmospheres [1]. So 20% of water vapor was added to the furnace atmosphere, which for the rest was a mixture of 68% of N_2, 10% CO_2, 0.7% of O_2 and 1.4% of CO to reproduce the firing conditions in the gas fired industrial kiln. This was achieved by using a special vaporizer and by heating the supplies and the cooling water of the furnace to avoid condensation of water at the walls. The sample support was made of SiC ceramics according to the setup of the industrial firing process.

Dimensional changes of the samples were measured using an optical system. For it the contour of the sample was imaged on a CMOS camera by a telecentric lens. A resolution of 2 μm for dimensional measurements was achieved. Details of TOM are described elsewhere [2]. Fig. 2a shows shrinkage curves for different heating rates and Fig. 2b a magnified section at low temperatures with the endothermic ($\Delta H = 190$ kJ/kg) dehydroxylation of kaolinite, the quartz inversion and the exothermic ($\Delta H = 38$ kJ/kg) decomposition of metakaolinite. Besides their influence on heat balance these reactions cause volumetric changes. Both effects have to be considered in the simulation of the temperature and stress field. Moreover, the dehydroxylation leads to overpressure, which depends on the gas flow within the pore system.

The specific heat and the heat of reaction have been measured using customary differential scanning calorimetry (DSC). Gas permeation was measured at room temperature by recording the reduction of an initially applied pressure gradient. The intrinsic permeability was 5.24×10^{-15} m^2. Young's modulus was determined at ambient temperature by ultrasonic velocity measurements using quenched samples. It increased linearly from 5.8 GPa for green samples to 8.7 GPa for samples heated to 1000 °C. Above that temperature Young's modulus was derived by interpolation between the values at 1000 °C and the Young's modulus of dense porcelain samples (90 GPa) according to the fractional density. The bending strength of quenched samples was measured at ambient temperature and at elevated temperature. Independent of measuring temperature, it was (5 ± 1) MPa until 900 °C where a steep increase was observed.

Creep was measured by positioning the sample between two vertical punches (Fig. 3a). They were uniaxially compressed by a small motor using a proportional rotary solenoid. The motor was mounted outside the thermal insulation of the heating zone within the vacuum tight housing of the furnace. To avoid caking between sample and punches, the sample was placed between two additional green compacts from the same mixture. Radial shrinkage was measured from the diameter of the sample at the centre and axial shrinkage was measured from the vertical distance of the two additional green compacts, which had a larger diameter than the sample (Fig. 3a). Only small forces between 1.25 and 6.6 N corresponding to initial stresses of 16 and 85 kPa respectively, were applied to avoid disturbance of the sintering process. Fig. 3b shows the superposition of radial and axial shrinkage and creep during sintering of the green samples. (Holding periods at the onset and at the end of shrinkage were introduced to obtain accurate data in temperature regions where creep was very small.)

Heat flow within the sample was measured using the well known laser-flash technique [3]. The front side of the sample was heated by a short laser pulse and the temperature was

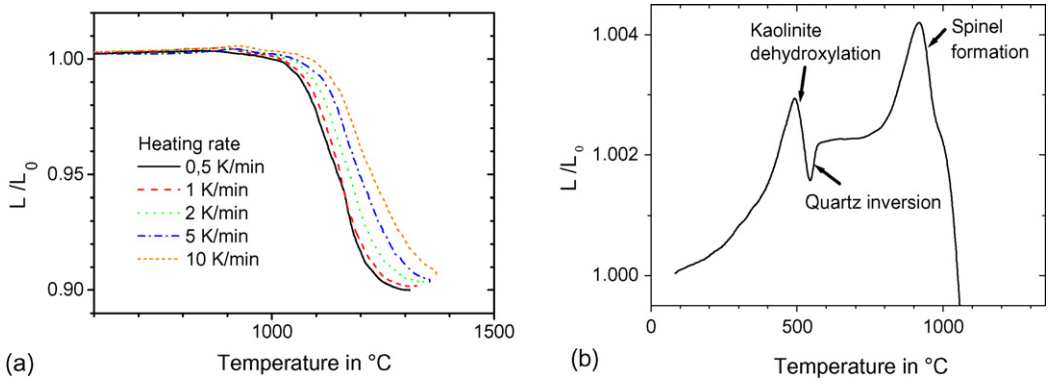

Fig. 2. Thermal diffusivity α of green and sintered AlN samples versus temperature.

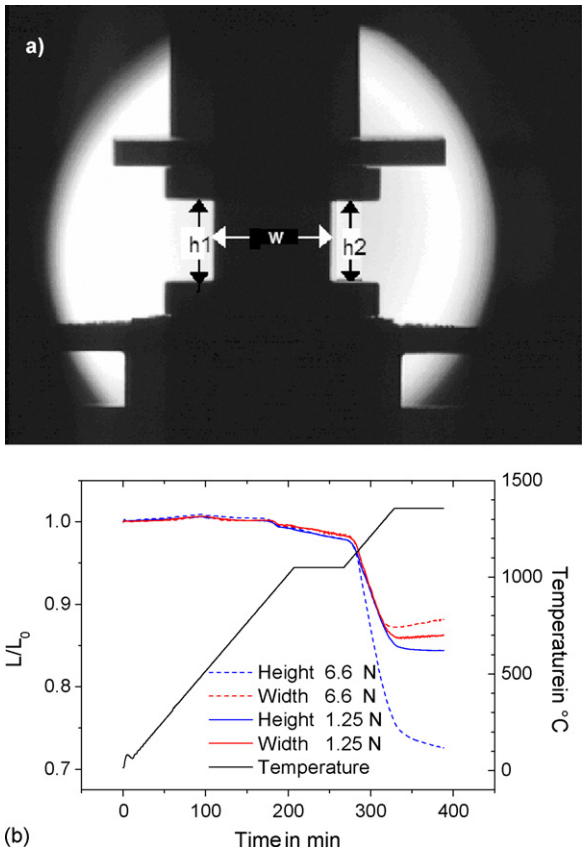

Fig. 3. Difference in dimensional change $\Delta L/L_0$ of green samples and reference samples where binder had been already removed.

monitored at its back side by a pyrometer (compare Fig. 1). Thermal diffusivity and the coefficient of heat transfer were obtained from the measured data by an inverse modeling procedure using a Finite Element program (ANSYS®). Details of the laser-flash measuring method were given elsewhere [2]. Fig. 4 shows the thermal diffusivities and coefficients of heat transfer during heating of a green sample. Thermal diffusivity starts from very small values below 0.6 mm^2/K and decreases until 850 °C which is attributed to increased phonon–phonon scattering. Then thermal diffusivity increases due to sintering

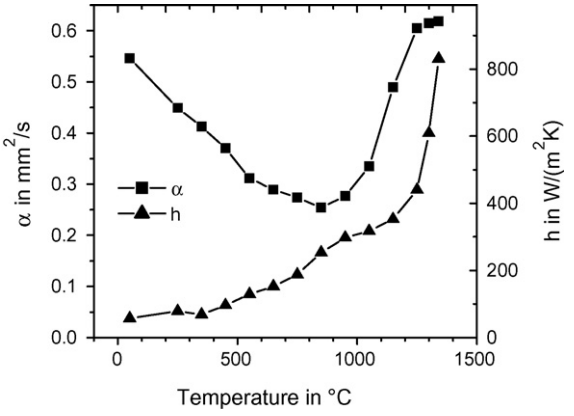

Fig. 4. FTIR spectrum of gaseous species evolved during binder pyrolysis of AlN green parts at 310 °C.

Fig. 5. (a) Weight loss of large-volume AlN green parts heated with different heating rates, (b) weight loss rate d (M/M_0)/dt versus weight loss $\Delta M/M_0$ at a heating rate of 5 K/min.

effects, which outweigh the scattering processes. The coefficient of heat transfer increases with increasing temperature due to an enhanced contribution of heat radiation.

3. Data evaluation and simulation of temperature and stress fields

The reaction data for the dehydroxylation and decomposition of kaolinite and metakaolinite respectively were obtained from the width and temperature shift of the corresponding peaks using constant heating rates and first order reaction kinetics. The activation energies were 520 and 1080 kJ/mol, respectively. For the dehydroxylation actually a Gaussian distribution of activation energies was used to meet the experimental data. This was attributed to structural disorder of the kaolinite.

The high voltage insulator had a height of 1700 mm and a strut diameter of 300 mm (Fig. 5). Due to its longish shape axial gradients were neglected and the insulator was represented in a

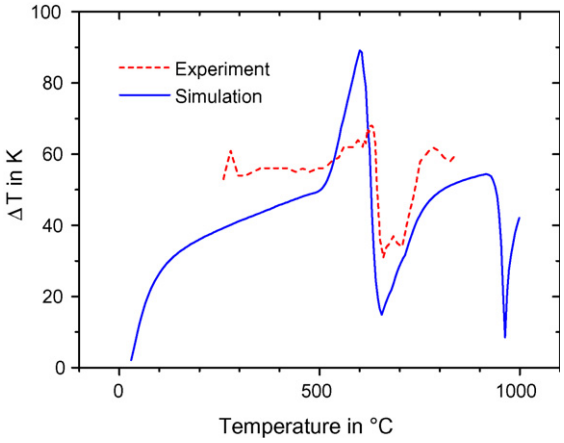

Fig. 6. (a) Kinetic field for the debinding of AlN green parts (straight lines are isoweightloss-lines) and (b) activation energy E derived from the slope of the isoweightloss-lines.

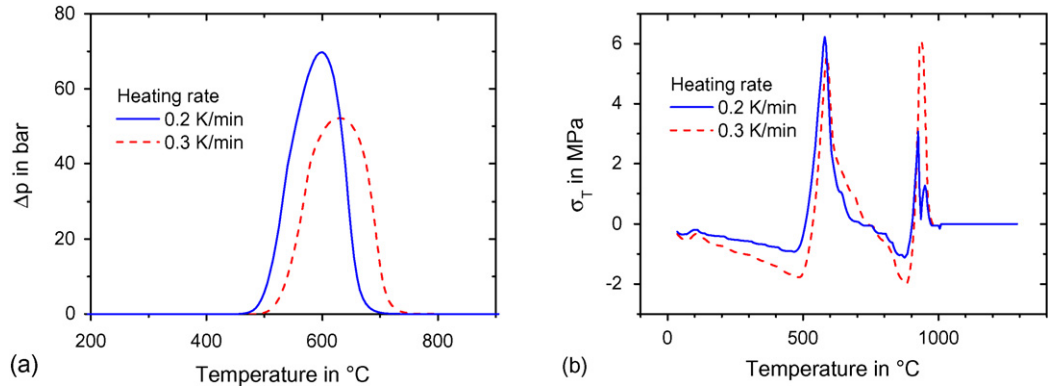

Fig. 7. (a) Silhouette of binder droplets on AlN substrate at a temperature of 160°C and (b) 280°C (heating rate 0.5 K/min).

finite element model by a simple disk of 300 mm diameter with plane strain and without axial heat or gas flow. The temperature dependence of the measured material properties was considered in the model by parameterization using simple functions like polynomials.

Heating was simulated in small temperature steps of 5 K. For each step temperatures were calculated first, considering heat transfer at the insulator surface from the furnace, heat of kaolinite reactions and local thermal diffusivity. Fig. 6 shows a comparison of the measured temperature gradient and the simulated gradient in a typical heating experiment. A reasonable agreement between experiment and simulation was obtained. Note that no fitted parameters have been used in the simulation. (The decrease of the temperature gradient at 600 °C is caused by a smaller heating rate in that temperature range). After the thermal simulation the production of water vapor according to the dehydroxylation reaction was calculated. The flow of water vapor within the pore channels was determined by a finite difference method from the measured permeability considering the effect of temperature on gas viscosity according to the Darcy equation [4]. Fig. 7a shows the overpressure at the centre axis of the insulator for different heating rates. A very high overpressure up to 70 bar was obtained. Overpressure can explain for the differences between experimental and measured temperatures (Fig. 6) since the effect of pressure on the kinetics of the dehydroxylation reaction was not included in the simulation.

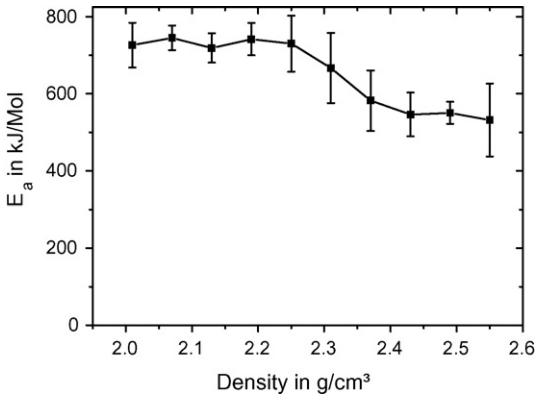

Fig. 8. Wetting angle Θ of binder on AlN substrate measured with different heating rates.

Finally the stresses were simulated using the local temperatures, the respective instantaneous coefficients of thermal expansion and the overpressure determined previously. Below the onset temperature for sintering (1000 °C) stresses were calculated in a linearly elastic model. Due to the volume changes caused by the various reactions, the stress distribution within the insulator changed completely during heating from 300 to 1000 °C. This was exemplified in Fig. 7b showing the hook stress at the surface of the insulators (tensile stresses were represented by a positive sign). Note that an increase of heating rate did not necessarily lead to enhanced overpressure or larger stresses (Fig. 7). This was attributed to the higher temperature gradient, which led to a distribution of the dehydroxylation reaction over a larger temperature range. At temperatures above 1000 °C sintering was considered using a viscoelastic model. Sintering kinetics was calculated from the shrinkage curves (Fig. 2a) using the kinetic field method [5]. The respective activation energies are shown in Fig. 8. A slight decrease of the activation energy was observed which was attributed to a decrease of the viscosity of the melt with increasing temperature leading to larger shrinkage rates.

From the sintering experiments with uniaxial load (Fig. 3) the viscous bulk and shear moduli were determined according to the method described in [6]. Using the viscous bulk moduli sintering stresses were calculated inversely by the requirement of obtaining the shrinkage, which was predicted by the kinetic field. These stresses were applied as additional local pressure loads in the FE simulation. Then the viscoelastic displacements were determined for the respective temperature step. After the onset of sintering, all stresses strongly decreased (Fig. 7b). This was attributed to creep which can compensate thermal stresses. The temperature time cycle has been varied in the simulations to identify shorter heating processes without increasing maximum stresses.

4. Conclusions

Using the present model a reduction of the heating cycle of the high voltage insulators by 40% (cold to cold) compared to the established heating cycle was obtained. The heating cycle

has already been implemented in industrial production of the insulators without any problems. A considerable increase in throughput and savings in energy were achieved. Although the effort of measuring was rather high, the advantage of larger production efficiency predominates. The experimental data used in the simulation were specific for the special type of green compact but they can be applied to any shape of the insulators.

The combination of in situ measurements and simulation presented for the high voltage insulator can readily be applied to the firing process of other large ceramic components.

Acknowledgements

The present study was supported by the federal state of Bavaria within a joint project on rapid sintering processes. The authors thank G. Fassbinder and A. Kammerer from company Lapp Insulator for providing the porcelain green samples, the strength and DSC data and verifying the sintering experiments. They also acknowledge the help of H. Schömig and C. Klinge with the measurements.

References

[1] C. Dannert, B. Durschang, F. Raether, F. Becker Materials Week 2000, Munich, Germany, Symp. 13 Process Development, www.materialsweek.org, 2000.
[2] J. Baber, A. Klimera, F. Raether, J. Eur. Ceram. Soc. 27 (2007) 701–705.
[3] W.J. Parker, R.J. Jenkins, C.P. Butler, G.L. Abbott, J. Appl. Phys. 32 (1961) 1679.
[4] H. Martin (Ed.), VDI-Wärmeatlas, Springer-Verlag, Berlin, 2002.
[5] H. Palmour, in: D. Uskokovic, H. Palmour, R.M. Spriggs (Eds.), Science of Sintering, Plenum Press, New York, 1989, p. 337.
[6] K.R. Venkatachari, R. Raj, J. Am. Ceram. Soc. 69 (1986) 499.